Journal of Molecular Structure 1234 (2021) 130145

Contents lists available at ScienceDirect

Journal of Molecular Structure

journal homepage: www.elsevier.com/locate/molstr

Synthesis, spectral, stereochemical, biological, molecular docking and DFT studies of 3-alkyl/3,5-dialkyl-2r,6c-di(naphthyl)piperidin-4-one picrates derivatives

S. Savithiri[a,*], S. Bharanidharan[b], P. Sugumar[c], C. Rajeevgandhi[d], M. Indhira[e]

[a] Department of Chemistry, Karpagam Academy of Higher Education, Coimbatore, 641 021, Tamilnadu, India
[b] Department of Physics, PRIST University, Puducherry, 605 007, India
[c] Department of Physics, Dhaanish Ahmed College of Engineering, Tambaram, Chennai, 601 301, Tamilnadu, India
[d] Department of Physics, Annai College of Arts and Science, Kumbakonam, 612503, Tamilnadu, India
[e] Department of Physics, Vivekanandha College of Arts and Sciences for Women (Autonomous), Tiruchengode, 637 205, Tamilnadu, India

ARTICLE INFO

Article history:
Received 10 December 2020
Revised 6 February 2021
Accepted 12 February 2021
Available online 26 February 2021

Keywords:
Picrates
FT-IR
NMR
Biological activity
DFT and Molecular docking studies

ABSTRACT

A new series of 3-alkyl/3,5-dialkyl-2r,6c-di(naphthyl)piperidin-4-one picrates (**1-6**) were synthesized their chemical structures were confirmed by elemental analysis, FT-IR, ^{1}H and ^{13}C NMR and mass spectral techniques and for compound **4** was characterized by HOMOCOSY, HSQC, HMBC, NOESY, and DEPT NMR spectral techniques. From the NMR spectral data, the observed chemical shifts and coupling constants suggested that compounds (**1-6**) adopt a normal chair conformation with equatorial orientation of all the naphthyl groups at C-2 and C-6 and alkyl group at C-3 and C-5 and from the ^{1}H chemical shifts H-5a and H-3a have a higher magnitude than H-5e. This is due to 1,3 diaxial interaction between axial NH proton and axial protons at C-3 and C-5. The synthesized compounds were screened for their bacterial activity against *Escherichia coli, Staphylococcus aureus, Bacillus.subtilis, Vibreo cholerae and Pseudomonas aeruginosa* and fungal activity against *Candida albicans, Aspergillus niger, Aspergillus flavus and Trichophyton rubrum.* All the compounds showed good antibacterial and antifungal activities. The optimized molecular structure of the synthesized compounds (**1-6**) were studied by using DFT/B3LYP/6-311++G(d,p) basis set. The calculated electrical dipole moment (μ) and first hyperpolarizability (βo) values shows that all the molecules might have nonlinear optical (NLO) behavior. The HOMO-LUMO transition implies that intra-molecular charge transfer takes place within the molecule. Molecular electrostatic potential (MEP) surface is used to understand the reactive sites of a molecule. To establish information about the molecular interactions between protein and this novel compound theoretically, docking studies were carried out in detail.

1. Introduction

Heterocyclic compounds play a vital role in biological processes and are widespread as natural products. Synthetically produced heterocycles designed by organic chemists are used, for instance, as Agrochemicals and pharmaceuticals and play an important role in human life. Among the family of heterocyclic compounds, nitrogen containing heterocyclic compounds, especially piperidine-4-ones presumably gaining considerable importance owing to varied biological properties such as antibacterial [1], antifungal [2], antiviral [3], anti-tumor [4], analgesic [5], anti-inflammatory, local anesthetic [6], Central Nervous System (CNS) and depressant activities [7]. The relative chemical shift order of equatorial and axial protons in the normal chair conformation of cyclohexane and its derivatives (deq > dax) are considered as caused by the magnetic anisotropic effect of the C-C single bonds. The influence of substituents on the chemical shifts of protons attached to the adjacent carbons has been studied in detail [8–10]. The effect of protonation on the ^{1}H and ^{13}C chemical shifts in 2r,6c-diphenylpiperidin-4-one by examining carefully their picrates [11]. By investigating one picrate with the corresponding hydrochloride [12], they have shown that anions also could influence ^{1}H chemical shifts. Various addition complexes were prepared using different heterocyclic nitrogen complexes with picric acid that exhibit NLO properties owing to hydrogen bonding and $\pi-\pi$ interactions [13,14]. Extensive effect is at present being expended to examine nonlinear optical materials that exhibit an array of potential applications in many fields of optical computing, telecommunications, optical power limiting, optical information processing and optical data storage [15-19]. Pi-

* Corresponding author.
E-mail address: savithiri.chem@gmail.com (S. Savithiri).

https://doi.org/10.1016/j.molstruc.2021.130145
0022-2860/

cric acid derivatives have charge transfer, due to the presence of phenolic OH favouring the formation of salts with various organic bases. Proton transfer complexes are intended for the development of first-order molecular hyperpolarizability (β) [20,21]. The bond formation process in picric acid complexes is due to the strength and nature of electron donor- acceptor type bonding. The linkage involves the formation of molecular complexes and electrostatic interactions. The formation of conjugated base, the picrates, and the value of molecular hyper polarizability is increased due to proton transfer [22]. In the present study, the synthesis of picrates characterized by spectral techniques and screens its anti-microbial activities and also has been carried out to identify the NLO property (first order hyperpolarizability), HOMO–LUMO energies and MEP analysis. In addition, molecular docking study has also been discussed in detail.

2. Experimental details

2.1. Materials and methods

All the solvents used were of spectral grade. The melting points of the compounds were measured in open capillaries and are uncorrected. IR spectra were recorded on an AVATAR-330 FT-IR spectrometer (Thermo Nicolet) using KBr (pellet form). ^{1}H NMR spectra were recorded at 400 MHz and ^{13}C NMR spectra at 100 MHz on a BRUKER model using DMSO-d6 as solvent for all the compounds. Tetramethylsilane (TMS) was used as internal reference for all NMR spectra, with chemical shifts reported in ((δ units parts per million) relative to the standard. ^{1}H NMR splitting patterns are designated as singlet (s), doublet (d), a doublet of doublet (dd), triplet (t), quartet (q) and multiplet (m). Coupling constants are expressed in Hertz (Hz). Mass spectra were recorded in VARIAN-SASTURAN 2200 GC–MS spectrometry using electron impact technique. The sample was prepared by dissolving about 1 mg in 5 ml of methanol. Microanalyses were performed on VarioMicro V2.2.0 CHN analyzer. Microbial screening studies were made at the Centre for biological sciences in Pondicherry.

2.2. Synthesis procedure of 3-alkyl/3,5-dialkyl-2r,6c-di(naphthyl) piperidin-4-one picrates

The piperidinium picrates (**1–6**) were prepared by mixing equimolar solutions of the corresponding 3-alkyl and 3,5-dialkyl-2r,6c-di(naphthyl)piperidin-4-one [23] with picric acid in ethanol and stirring the solution for 30 mins. The yellowish crystals formed were filtered. The yield of the product was found to be 95%. The harvested crystals were crystallized repeatedly to get excellent quality crystals.

2.2a. 3t-*methyl*-2r,6c-*di(naphthalene-1-yl)piperidin-4-one picrate (1)*

Yield 85%; m.p.: 176-178 (°C); MF: $C_{32}H_{26}N_4O_8$; Elemental analysis: Calcd (%): C, (64.64; H, 4.41; N, 9.42; Found (%): C, 64.59; H, 4.33; N, 9.41; IR (KBr) (cm^{-1}): 3435 (N-H stretching), 3077-2990 (aromatic C-H stretching), 2930-2855 (aliphatic C-H stretching), 1713 (C=O stretching), 1620 (C=C stretching), 1435 (C-O stretching), 1557, 1489 (NO_2 asymmetric stretching), 1329, 1269 (NO_2 symmetric stretching), 1078 (C-N stretching), 783-708 (aromatic C-H out of plane bending vibration), 663 (aromatic C-C out of plane bending vibration); ^{1}H NMR (400 MHz, DMSO-d_6, δ, ppm): 10.30 (d, 1H, Ax-NH, J = 7.6 Hz), 10.62 (d, 1H, Eq-NH, J = 8.0 Hz), 8.59 (s, 2H, picryl ring), 7.59-8.55 (m, 14H, Ar-H), 6.23 (t, 1H, H-6a, J_{6a5a} = 10.4 Hz), 5.99 (t, 1H, H-2a, J_{2a3a} = 10 Hz), 3.76 (t, 1H, H-3a & H-5a), 2.91 (d, 1H, H-5e, J_{5a5e} = 15.2 Hz), 0.81 (d, 3H, CH_3); ^{13}C NMR (100 MHz, DMSO-d_6, δ, ppm): 203.65 (C=O), 122.51-141.74 (Ar-C), 160.80 (C-O), 58.01 (C-2), 54.20 (C-6), 47.46 (C-3), 44.85 (C-5), 10.10 (CH_3). Mass (m/z)**:** 594.8

2.2b. 3t-*isopropyl*-2r,6c-*di(naphthalene-1-yl)piperidin-4-one picrate (2)*

Yield 87%; m.p.: 172-174 (°C); MF: $C_{34}H_{30}N_4O$; Elemental analysis: Calcd (%): C, 65.59; H, 4.86; N, 9.00; Found (%):C, 65.35; H, 4.78; N, 9.03; IR (KBr) (cm^{-1}): 3418 (N-H stretching), 3092-2967 (aromatic C-H stretching), 2934-2870 (aliphatic C-H stretching), 1711 (C=O stretching), 1626 (C=C stretching), 1437 (C-O stretching), 1555, 1491 (NO_2 asymmetric stretching), 1337, 1271 (NO_2 symmetric stretching), 1082 (C-N stretching), 787-710 (aromatic C-H out of plane bending vibration), 663(aromatic C-C out of plane bending vibration); ^{1}H NMR (400 MHz, DMSO-d_6, δ, ppm): 9.64 (d, 1H, Ax-NH, J = 10 Hz), 10.40 (d, 1H, Eq-NH, J = 9.2 Hz), 8.60 (s, 2H, picryl ring), 7.59-8.57 (m, 14H, Ar-H), 6.27 (t, 1H, H-6a, J_{6a5a} = 10.8 Hz), 6.12 (t, 1H, H-2a, J_{2a3a} = 10.4 Hz), 3.55 (t, 1H, H-3a & H-5a), 2.88 (d, 1H, H-5e, J_{5a5e} = 15.2 Hz), 1.66 (t, 1H, CH), 0.76 (d, 3H, CH_3), 1.02 (d, 3H, CH_3); ^{13}C NMR (100 MHz, DMSO-d_6, δ, ppm): 203.23 (C=O), 122.93-141.74 (Ar-C), 160.60 (C-O), 56.02 (C-2), 55.89 (C-6), 53.53 (C-3), 45.76 (C-5), 25.83 (CH), 20.53, 17.54 (CH_3).

2.2c. 3,5-*dimethyl*-2r,6c-*di(naphthalene-1-yl)piperidin-4-one picrate (3)*

Yield 75%; m.p.: 106-108 (°C); MF: $C_{33}H_{28}N_4O_8$; Elemental analysis: Calcd (%): C, 65.13; H, 4.64; N, 9.21; Found (%):C, 65.01; H, 4.53; N, 9.15; IR (KBr) (cm^{-1}): 3420 (N-H stretching), 3078-2992 (aromatic C-H stretching), 2926-2853 (aliphatic C-H stretching), 1713 (C=O stretching), 1622 (C=C stretching), 1446 (C-O stretching), 1549, 1489 (NO_2 asymmetric stretching), 1329, 1271 (NO_2 symmetric stretching), 1076 (C-N stretching), 783-712 (aromatic C-H out of plane bending vibration), 605 (aromatic C-C out of plane bending vibration); ^{1}H NMR (400 MHz, DMSO-d_6, δ, ppm): 9.55 (d, 1H, Ax-NH, J = 9.6 Hz), 10.33 (d, 1H, Eq-NH, J = 8.8 Hz), 8.59 (s, 2H, picryl ring), 7.58-8.44 (m, Ar-H), 5.96 (t, 1H, H-6a & H-2a, $J_{6a5a\ \&\ 2a3a}$ = 10.8 Hz), 3.69 (q, 1H, H-3a & H-5a, J = 11.6 Hz), 0.83 (d, 6H, CH_3); ^{13}C NMR (100 MHz, DMSO-d_6, δ, ppm): 205.28 (C=O), 122.80-141.75 (Ar-C), 160.76 (C-O), 57.71 (C-2 & C-6), 47.01 (C-3) & C-5), 10.46 (CH_3); Mass (m/z): 609.8 (m+1)

2.2d. 3t-*butyl*-2r,6c-*di(naphthalene-1-yl)piperidin-4-one picrate (4)*

Yield 80%; m.p.: 150–152 (°C); MF: $C_{35}H_{32}N_4O_8$; Elemental analysis: Calcd (%): C, 66.03; H, 5.07; N, 8.80; Found (%):C, 66.01; H, 4.99; N, 8.76; IR (KBr) (cm^{-1}): 3435 (N-H stretching), 3078-2957 (aromatic C-H stretching), 2928-2862 (aliphatic C-H stretching), 1721 (C=O stretching), 1611 (C=C stretching), 1433 (C-O stretching), 1559, 1489 (NO_2 asymmetric stretching), 1335, 1269 (NO_2 symmetric stretching), 1080 (C-N stretching), 777-710 (aromatic C-H out of plane bending vibration), 612 (aromatic C-C out of plane bending vibration); ^{1}H NMR (400 MHz, DMSO-d_6, δ, ppm): 9.77 (d, 1H, Ax-NH, J = 8.4 Hz), 10.34 (d, 1H, Eq-NH, J = 7.2 Hz), 8.59 (s, 2H, picryl ring), 7.60-8.47 (m, 14H, Ar-H), 6.23 (t, 1H, H-6a, J_{6a5a} = 10.8 Hz), 6.03 (t, 1H, H-2a, J_{2a3a} = 9.6 Hz), 3.44 (q, 1H, H-3a), 3.58 (q, 1H, H-5a, J_{5a5e} = 14.0 Hz), 2.91 (d, 1H, H-5e), 0.90-1.52 (m, 6H, CH_2), 0.56 (t, 3H, CH_3). ^{13}C NMR (100 MHz, DMSO-d_6, δ, ppm): 203.40 (C=O), 122.58-141.62 (Ar-C), 160.85 (C-O), 56.72 (C-2), 53.95 (C-6), 51.51 (C-3), 45.05 (C-5), 21.85-28.43 (CH_2), 13.30 (CH_3).

2.2e. 3t-*pentyl*-2r,6c-*di(naphthalene-2-yl)piperidin-4-one picrate (5)*

Yield 78%; m.p.: 156-158 (°C); MF: $C_{36}H_{28}N_4O_8$; Elemental analysis: Calcd (%): C, 66.45; H, 5.57; N, 8.61; Found (%):C, 66.35; H,

5.46; N, 8.57; IR (KBr) (cm^{-1}): 3429 (N-H stretching), 3084-2953 (aromatic C-H stretching), 2928-2860 (aliphatic C-H stretching), 1719 (C=O stretching), 1622 (C=C stretching), 1435 (C-O stretching), 1558, 1485 (NO_2 asymmetric stretching), 1329, 1269 (NO_2 symmetric stretching), 1078 (C-N stretching), 787-710 (aromatic C-H out of plane bending vibration), 664 (aromatic C-C out of plane bending vibration); ^{1}H NMR (400 MHz, DMSO-d_6, δ, ppm): 10.15 (s, 1H, Ax-NH), 10.15 (s, 1H, Eq-NH), 8.59 (s, 2H, picryl ring), 7.59-8.22 (m, Ar-H), 5.24 (t, 1H, H-6a, J_{6a5a} = 12.8 Hz), 4.97 (t, 1H, H-2a, J_{2a3a} = 9.6 Hz), 3.43 (t, 1H, H-3a), 3.68 (t, 1H, H-5a, J_{5a5e} = 14.4 Hz), 2.89 (d, 1H, H-5e), 1.06-1.47 (m, 8H, CH_2), 0.70 (t, 3H, CH_3); ^{13}C NMR (100 MHz, DMSO-d_6, δ, ppm): 203.30 (C=O), 124.38-141.73 (Ar-C), 160.74 (C-O), 63.38 (C-2), 59.00 (C-6), 50.43 (C-3), 44.53 (C-5), 21.56-31.13 (CH_2), 13.59 (CH_3).

2.2f. 3t-methyl-2r,6c-di(naphthalene-2-yl)piperidin-4-one picrate (6)

Yield 85%; m.p.: 182-184 (°C); MF: $C_{32}H_{26}N_4O_8$; Elemental analysis: Calcd (%): C, 64.64; H, 4.41; N, 9.42; Found (%):C, 64.20; H, 4.31; N, 9.28; IR (KBr) (cm^{-1}): 3426 (N-H stretching), 3084 (aromatic C-H stretching), 2928-2855 (aliphatic C-H stretching), 1707 (C=O stretching), 1624 (C=C stretching), 1433 (C-O stretching), 1559, 1487 (NO_2 asymmetric stretching), 1333, 1269 (NO_2 symmetric stretching), 1078 (C-N stretching), 777-708 (aromatic C-H out of plane bending vibration), 667 (aromatic C-C out of plane bending vibration), ^{1}H NMR (400 MHz, DMSO-d_6, δ, ppm): 9.76 (d, 1H, Ax-NH, J = 8.8 Hz), 10.11 (d, 1H, Eq-NH, J = 8.8 Hz), 8.58 (s, 2H, picryl ring), 7.69-8.18 (m, Ar-H), 5.24 (t, 1H, H-6a, J_{6a5a} = 10.0 Hz), 4.91 (q, 1H, H-2a, J_{2a3a} = 2.4 Hz), 3.52 (m, 1H, H-3a & H-5a), 2.93 (d, 1H, H-5e, J_{5a5e} = 14.4 Hz), 0.86 (d, 3H, CH_3); ^{13}C NMR (100 MHz, DMSO-d_6, δ, ppm): 203.41 (C=O), 122.24-141.73 (Ar-C), 160.73 (C-O), 64.45 (C-2), 58.78 (C-6), 45.79 (C-3), 43.88 (C-5), 10.44 (CH_3).

2.3a. Antibacterial activity by disc diffusion method

Nutrient agar plates were prepared under sterile conditions and incubated overnight to detect contamination. About 0.2 ml of working stock cultures was transferred into separate nutrient agar plates and spread thoroughly using a glass spreader. Whatmann No. 1 disc (6 mm in diameter) was impregnated with the test compounds dissolved in DMSO (200 mg/ml) for about half an hour. Commercially available drug disc (Ciprofloxacin 10 lg/disc) was used as positive reference standard. Negative controls were also prepared by impregnating the disc of the same size in DMSO solvent. The discs were placed on the inoculated agar plates and incubated at 37 ± 1°C for about 18–24 h. Antibacterial activity was evaluated by measuring the zone of inhibition against the test organism.

2.3b. Antifungal activity by disc diffusion method

Sabouraud's dextrose agar (SDA) medium was used for the growth of fungi and testing was done in Sabouraud's dextrose broth (SDB) medium. The subculture and the viable count were carried out by the same procedure used in antibacterial studies except the temperature, which was maintained at 28 ± 1°C for about 72 h. Similarly for disc diffusion method, the petri dishes were incubated at 28 ± 1°C for about 72 h. The same concentration of the test compound, solvent (DMSO) and Cetramazole (standard) prepared previously were used for the antifungal studies.

2.3c. Minimum inhibitory concentration (MIC)

The lowest concentration of the test compounds which caused apparently the inhibition of growth of organism, was taken as the minimum inhibitory concentration. The MIC was recorded by visual observation after 24 h (bacteria) and 72–96 h (fungi) of incubation. The sterile distilled water and DMSO did not show any inhibition.

2.4. Computational details

The Density Functional Theory (DFT) with B3LYP level theory using 6-311++G(d,p) basis set in Gaussian-09 have been used for theoretical calculations [24]. Following the geometry optimizations with B3LYP method, HOMO and LUMO energy values and energy gap for compounds **(1-6)** were calculated by using B3LYP method with 6-311++G(d,p) basis set. Molecular Electrostatic Potentials (MEPs) of compounds **(1-6)** were plotted in 3D by using optimized structures at B3LYP/6-311++G(d,p) level theory. Furthermore, in order to show nonlinear optical (NLO) activity of title molecule, the dipole moment, linear polarizability and first order hyperpolarizability were obtained from molecular polarizabilities based on theoretical calculations. Acetylcholinesterase (AChE), an enzyme present in the neuromuscular junctions and responsible for the hydrolysis of the neurotransmitter acetylcholine. Three-dimensional crystal structures of TcAChE complexes were retrieved from the RCSB (Research Collaboratory for Structural Bioinformatics) protein data bank under PDB ID: 1EVE [25]. The active site of TcAChE was defined as the collection of residues within 15.0 Å of the bound inhibitor present in the reference structure 1ACJ. The bound inhibitors were not included in the docking runs. Docking calculations were carried out on Acetylcholinesterase Inhibitors enzyme protein model [26]. Essential hydrogen atoms, Kollman united atom type charges, and solvation parameters were added with the aid of AutoDock tools [27].

3. Results and discussion

3-alkyl/3,5-dialkyl-2r,6c-di(naphthyl)piperidin-4-one picrates derivatives, according to the synthetic sequences of reactions illustrated in Scheme 1. The structures of all the synthesized compounds (**1-6**) are established on the basis of FT-IR, ^{1}H and ^{13}C NMR and mass spectral techniques and for compound **4** in addition to the 2D NMR (HOMOCOSY, HSQC, HMBC, NOESY, and DEPT) spectral studies were performed to make unambiguous configurationals and conformationals characterizations.

3.1. IR spectral analysis

In the IR spectrum of **4**, the prominent peaks around 3435 and 1721 cm^{-1} are attributed to NH and C=O vibrational modes, respectively. The C=C stretching vibration of the naphthyl ring appeared around 1611 cm^{-1}. The C-N stretching mode of the piperidine ring appeared around 1080 cm^{-1}. The peaks around 777-710 cm^{-1} are attributed to aromatic C-H out of plane bending vibrations. The NO_2 asymmetric stretching vibration of picryl group appeared around 1559-1489 cm^{-1}. The peaks around 1335-1269 cm^{-1} are due to NO_2 symmetric stretching, vibration modes of picryl group. The peak around 1433 cm^{-1} is attributed to C-O vibrational mode of picryl group. The FT-IR spectral data of compound **1-6** are given in Table 1. It is seen that the IR frequencies are influenced by the substitutes in the aromatic ring.

3.2. NMR spectral analysis

In the ^{1}H NMR spectrum of **4** is shown in Fig. 1, the two doublets at 9.77 ppm (J = 8.4 Hz) and 10.34 ppm (J = 7.2 Hz) are assigned to NH axial and equatorial protons of piperidinium amino group. The picryl protons at 8.59 ppm correspond to two proton

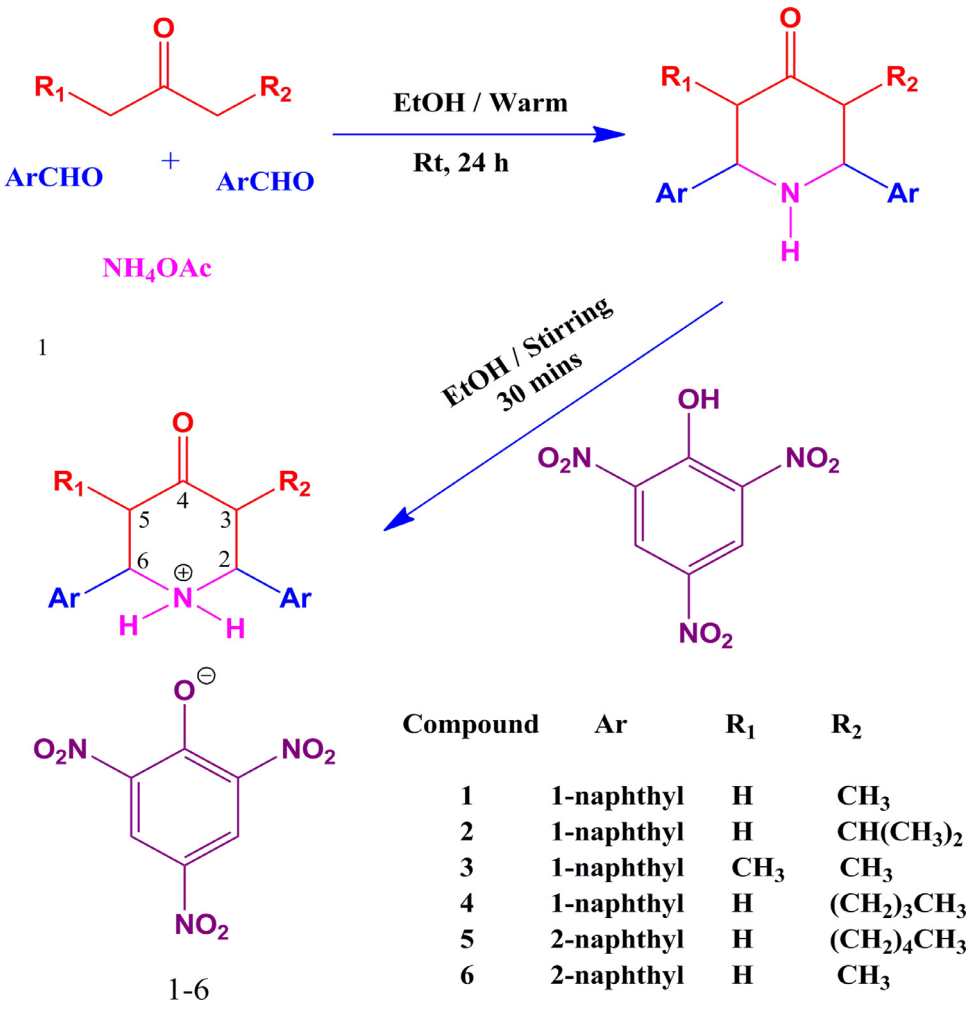

Compound	Ar	R_1	R_2
1	1-naphthyl	H	CH_3
2	1-naphthyl	H	$CH(CH_3)_2$
3	1-naphthyl	CH_3	CH_3
4	1-naphthyl	H	$(CH_2)_3CH_3$
5	2-naphthyl	H	$(CH_2)_4CH_3$
6	2-naphthyl	H	CH_3

Scheme 1. Synthetic route for 3-alkyl /3,5-dialkyl-2r,6c-di(naphthyl)piperidin-4-one picrates derivatives.

Table 1
IR spectral data of compounds (1-6).

1	2	3	4	5	6	Assignments
3435	3418	3420	3435	3429	3426	NH
3077-2990	3092-2967	3078-2992	3078-2957	3084-2953	3084	C-H
2930-2855	2934-2870	2926-2853	2928-2862	2928-2860	2855	
1713	1711	1713	1721	1719	1707	C=O
1078	1082	1076	1080	1078	1078	C-N
1620	1626	1622	1611	1622	1624	C=C
1435	1437	1446	1433	1435	1433	C-O
1557	1555	1549	1559	1558	1559	NO_2 asymmetric stretching
1489	1491	1489	1489	1485	1487	
1329	1337	1329	1335	1329	1333	NO_2 symmetric stretching
1269	1271	1271	1269	1269	1269	
783-708	787-710	783-712	777-710	787-710	777-708	Aromatic C-H out of plane bending vibrations
663	663	605	612	664	667	Aromatic C-C out of plane bending vibrations

integral values. All the aromatic protons are observed in the region 7.59-8.47 ppm. The two triplets observed at 6.03 and 6.23 ppm are due to bezylic protons at C-2 and C-6 respectively. The axial methylene proton H-5a appears as a quartet at 3.58 ppm and the equatorial methylene proton H-5e is observed at 2.91 ppm. The axial methine proton H-3a appears as a quartet at 3.44 ppm. From the ^{1}H chemical shifts H-5a and H-3a have a higher magnitude than H-5e. This is due to 1,3 diaxial interaction between axial NH proton and the axial protons at C-3 and C-5. The signal at 0.81 ppm is due to methyl protons at C-3 of piperidone moiety. In the protonated piperidine-4-one derivatives, the axial NH bond experiences severe *syn* 1,3-diaxial interaction with the axial protons at C-5 and C-3 and due to these interactions the protons are deshielded to a greater extent than the corresponding C-3 and C-5 carbons which are shielded. The ^{1}H chemical shift values are summarized in Table 2. The assignments are further confirmed by HOMOCOSY and NOESY correlation spectra of compound **4**.

In order to determine the effect of protonation on chemical shifts, the chemical shifts of 2,6-dinaphthylpicrates **1** and **5** were compared with the corresponding piperidin-4-ones and 2,6-diphenylpicrates. Data in Table 5 reveals that picrate formation deshields H-2a and H-6a to a greater extent. In the picrate deriva-

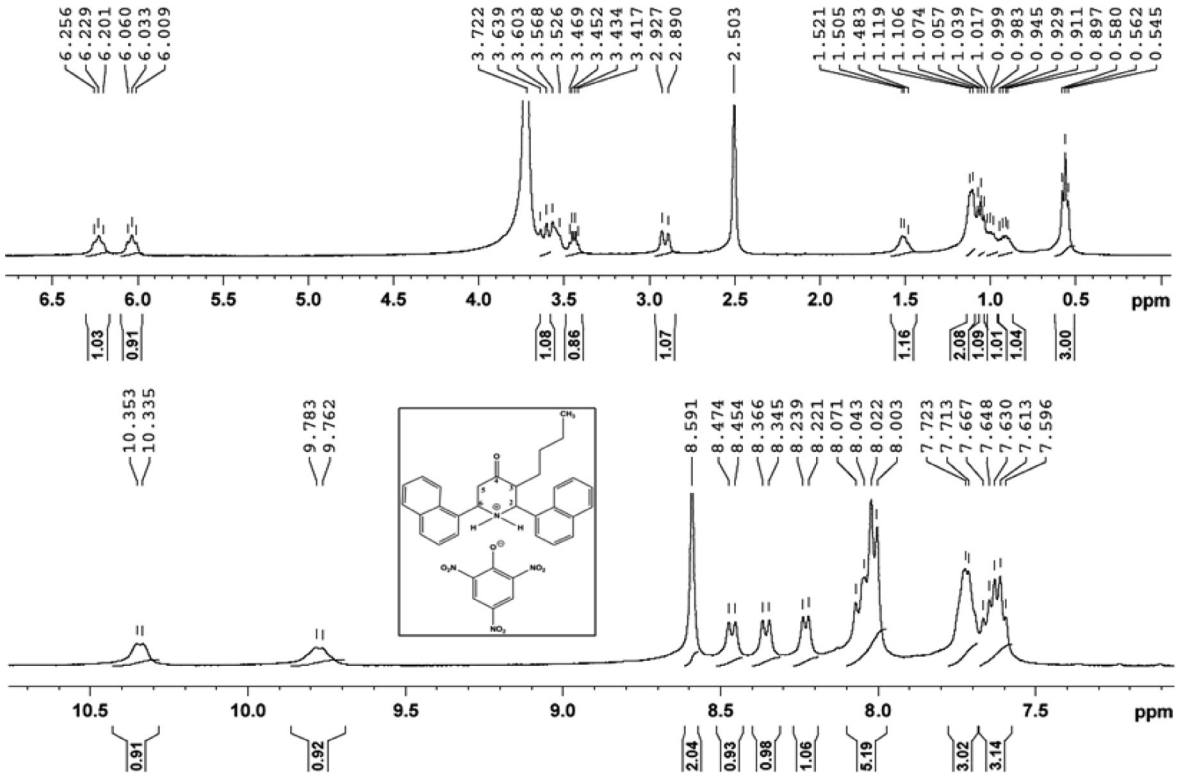

Fig. 1. ^{1}H NMR Spectrum of compound 4.

Table 2
^{1}H chemical shifts (ppm) of compounds (1–6).

Compound	H-2a	H-6a	H-5a	H-5e	H-3a	Ax-NH	Eq-NH	CH	CH_2	Picryl ring	CH_3	Aromatic Protons
1	5.99	6.23	3.76	2.91	3.76	10.30	10.62	-	-	8.59	0.81	7.59-8.55
2	6.12	6.27	3.55	2.88	3.55	9.64	10.40	1.66	-	8.60	0.76, 1.02	7.59-8.57
3	5.96	5.96	3.69	-	3.69	9.55	10.33	-	-	8.59	0.83	7.58-8.44
4	6.03	6.23	2.91	3.58	3.44	9.77	10.34	-	0.89-1.52	8.59	0.56	7.60-8.47
5	4.97	5.24	2.89	3.68	3.43	10.15	10.15	-	1.06-1.47	8.59	0.70	7.59-.822
6	4.91	5.24	3.52	2.93	3.52	9.76	10.11	-	-	8.58	0.86	7.69-8.18

tives the two protons at nitrogen occupy axial and equatorial orientations. The magnetic anisotropic effect of the axial N-H bond is responsible for the greater downfield shift observed on H-6a and H-2a in compound **4**. It is also seen that axial methylene proton H-5a is deshielded to a greater extent and it can be explained by syn 1,3-diaxial interaction. Picrate formation deshields the alkyl protons at C-3 also. NOESY spectrum of **4** is shown in Fig. 2. It is seen that NOE between H-2a and H-3a and that between H-6a and H-5 (i.e. H-5a and H-5e) are strong. The aromatic proton at 7.59 ppm should show strong NOE with H-3a and H-5a. Obviously, these protons must be the ortho protons of the naphthyl ring group at C-2 and C-6. Thus, the observed NOE of **4** supports the determined vicinal coupling constant. For compound **4** these assignments were confirmed by HSQC and HMBC spectra. The observed correlations in the HOMOCOSY, NOESY, HSQC and HMBC NOESY spectra are given in Table 4.

The compounds (**1-6**) should exist in chair conformation. In the chair conformation the aryl group alkyl group at C-3 are equatorial orientation. The coupling constant values and position of the chemical shifts were used to predict the conformation of the compound. The observation of large vicinal coupling constant values $^{3}J_{2a3a}$ = 9.6 and $^{3}J_{6a5a}$ = 10.8 Hz and small values of the vicinal coupling constant are not resolved. For the protons of C-6 and C-2 in **1-6** indicate that the six member heterocyclic rings adopts a normal chair conformation (Fig. 3) With equatorial orientation of aryl groups at C-2 and C-6 and alkyl group at C-3 and C-5. In compounds (**1-6**) the heterocyclic ring may be flattened or distorted about the (C-2)-(C-3) bond to decrease *gauche* interaction between the equatorial naphthyl groups and the equatorial alkyl group at C-2, C-6, C-3 and C-5 respectively.

In the ^{13}C NMR spectrum of compound **4** is shown in Fig. 4, the aromatic carbons are distinguished from other carbons by their characteristic absorptions at 122.58-141.62 ppm. The signal at 203.40 ppm in the most downfield is characteristic of carbonyl carbon. The signal in the downfield at 160.85 ppm is due to the C-O carbon of picryl group. The signals at 56.72 and 53.95 ppm are due to C-2 and C-6. The signals at 51.51 and 45.05 ppm are due to C-3 and C-5. The signal observed in the region 21.92-31.13 ppm are assigned to methylene carbons of butyl group at C-3 of piperidone ring and the most upfield signal at 13.30 ppm is assigned to methyl carbon of butyl group at C-3. The chemical shift values are reproduced in Table 3. It is clearly indicated that protonation shields all carbons. The shielding magnitude observed on C-3 and C-5 carbons is more that of C-2 and C-6 carbons. Due to protonation, the axial N-H bond experiences severe syn 1,3-diaxial interaction with axial hydrogens at C-3 and C-5 and due to these interactions butyl protons at C-3 and H-5a proton are shielded and the corresponding carbons are shielded. A ^{13}C NMR spectral study supported that the proposed chair conformation of the synthesized compounds with the equatorial orientation of the bulky aryl and

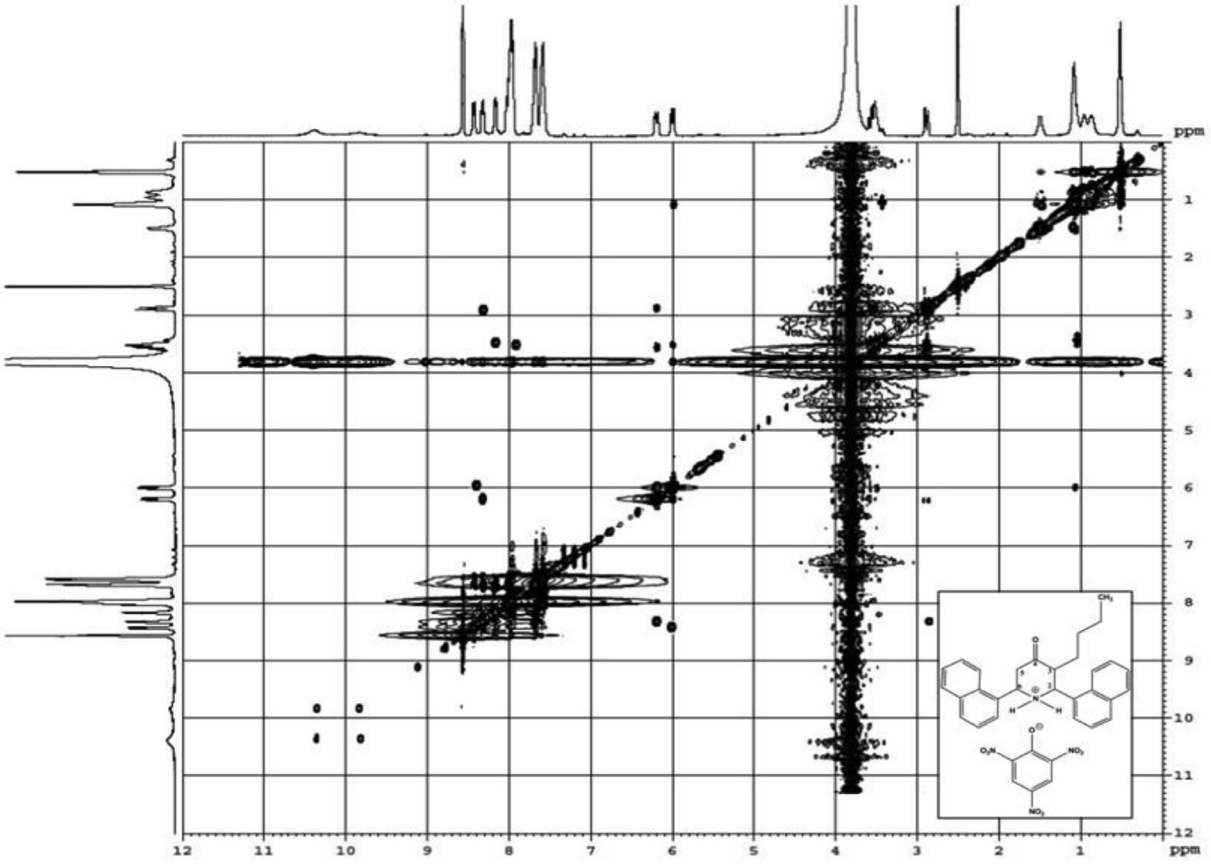

Fig. 2. NOESY Spectrum of compound 4.

Table 3
^{13}C chemical shifts (ppm) of compounds (1–6).

Compound	C-2	C-3	C-5	C-6	CH_2	CH	CH_3	C=O	C-O	Aromatic Carbons
1	58.01	47.46	44.85	54.20	-	-	10.10	203.65	160.80	122.51-141.74
2	56.02	53.53	45.76	55.89	-	25.83	20.53, 17.54	203.23	160.60	122.93-141.74
3	57.71	47.01	47.01	57.71	-	-	10.46	205.28	160.76	122.80-141.75
4	56.72	51.51	45.05	53.95	21.85-28.43	-	13.30	203.40	160.85	122.58-141.62
5	63.38	50.43	44.53	59.00	21.56-31.13	-	13.59	203.30	160.74	124.38-141.73
6	64.45	45.79	43.88	58.78	-	-	10.44	203.41	160.73	122.24-141.73

Table 4
Correlation in HOMOCOSY, NOESY, HSQC and HMBC spectra of compound 4 (δ, ppm).

^{1}H NMR Signal	Correlation in HOMOCOSY	Correlation in NOESY	Correlation in HSQC	Correlation in HMBC
6.23 (H-6a)	3.58 (H-5a), 2.91 (H-5e), 9.77 (Ax-NH)	3.58 (H-5a), 2.91 (H-5e), 7.59-8.47 (Aromatic Protons)	53.95 (C-6)	-
6.03 (H-2a)	3.44 (H-3a), 9.77 (Ax-NH)	3.44 (H-3a), 0.89-1.52 (CH_2), 7.59-8.47 (Aromatic Protons)	56.72 (C(2))	51.51 (C-3), α), 122.58-141.62 (Aromatic Carbons, α)
3.44 (H-3a)	0.89-1.52 (CH_2), 6.03 (H-2a)	0.89-1.52 (CH_2), 6.03 (H-2a), 7.59-8.47 (Aromatic Protons)	51.51 (C-3)	203.40 (C-4), α), 21.92-31.13 (CH_2, α), 122.58-141.62 (Aromatic Carbons, β)
3.58 (H-5a)	2.91 (H-5e), 6.23 (H-6a)	2.91 (H-5e), 6.23 (H-6a), 7.59-8.47 (Aromatic Protons)	45.05 (C-5)	53.95 (C-6), α), 203.40 (C-4), α), 122.58-141.62 (Aromatic Carbons, α)
2.91 (H-5e)	3.58 (H-5a), 6.23 (H-6a)	3.58 (H-5a), 6.23 (H-6a), 7.59-8.47 (Aromatic Protons)	45.05 (C-5)	203.40 (C-4), α)
0.56 (CH_3)	0.89-1.52 (CH_2),	0.89-1.52 (CH_2)	13.30 (CH_3)	21.92-31.13 (CH_2, α)
0.89-1.52 (CH_2)	0.89-1.52 (CH_2), 3.44 (H-3a)	0.89-1.52 (CH_2), 3.44 (H-3a), 6.03 (H-2a)	21.85-28.43 (CH_2)	21.85-28.43 (CH_2, α), 203.40 (C-4), β)
9.77 (Ax-NH)	10.34 (Eq-NH), 6.23 (H-6a), 6.03 (H-2a)	10.34 (Eq-NH), 3.58 (H-5a)	-	-
10.34 (Eq-NH)	9.77 (Ax-NH)	9.77 (Ax-NH), 3.58 (H-5a)	-	-
7.59-8.47 (Aromatic Protons)	7.59-8.47 (Aromatic Protons)	6.23 (H-6a), 6.03 (H-2a), 3.58 (H-5a), 2.91 (H-5e), 3.44 (H-3a),	122.58-141.62 (Aromatic carbons)	53.95 (C-6), α), 56.72 (C-2), α)

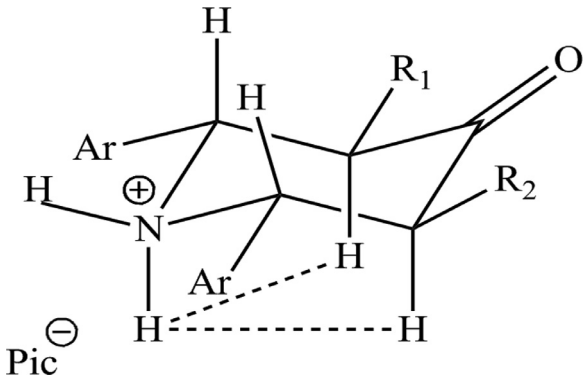

Fig. 3. Schematic representation of syn 1,3-diaxial interactions.

Table 5
^{1}H chemical shift difference between piperidones[a] and picrates (1) and phenyl picrates[b] and naphthyl picrates (5).

Compound 1 piperidones[a] and picrates		Compound 5 phenyl picrates[b] and naphthyl picrates
H(6)	0.26	-0.23
H(2)	-0.17	-0.23
H(5a)	-0.3	-0.04
H(3a)	-0.03	-0.45
H(5e)	0.4	-0.14
CH3	-0.01	0.04

[a] Taken from Ref. [28].
[b] Taken from Ref. [23].

alkyl groups. The ^{13}C chemical shifts of compounds **1** and **5** were compared with the corresponding piperidin-4-ones (Table 6). The assignments are further confirmed by using DEPT, HSQC and HMBC spectra.

Table 6
^{13}C chemical shift difference between piperidones[a] and picrates (1) and phenyl picrates[b] and naphthyl picrates (5).

Compound 1 piperidones[a] and picrates		Compound 5 phenyl picrates[b] and naphthyl picrates	
C(2)	0.80	C(2)	-0.37
C(3)	0.76	C(3)	-0.05
C(4)	0.68	C(4)	-0.16
C(5)	0.74	C(5)	-0.25
C(6)	-9.15	C(6)	-0.35
CH_3	0.49	CH_3	0.03

[a] Taken from Ref. [28].
[b] Taken from Ref. [23].

These compounds were further characterized by mass spectroscopy (Fig. S10 and Fig. S15) and the detected The mass spectra of compounds **1** and **3** were recorded and the observed m/z values are consistent with the proposed molecular formula of the respective compounds. The presence of peaks at m/z 594.8 and 609.8 are due to the molecular ion peaks of compounds **1** and **3**.

3.3. Antimicrobial activity

The preliminary antimicrobial activity of the compounds (**1-6**) was carried out using disc diffusion and two fold serial dilution methods. The bacterial strains viz., *Escherichia coli, Staphylococcus aureus, Bacillus.subtilis, Vibreo cholerae* and *Pseudomonas aeruginosa* and fungal strains viz., *Candida albicans, Aspergillus niger, Aspergillus flavus* and *Trichophyton rubrum* were used for this study. DMSO was used as control while *Ciprofloxacin* and *Amphotericin B* were used as standard drugs respectively for bacterial and fungal strains.

The zone of inhibition (mm) and minimum inhibitory concentrations (MIC in μg/mL) of the compounds **1-6** against the tested

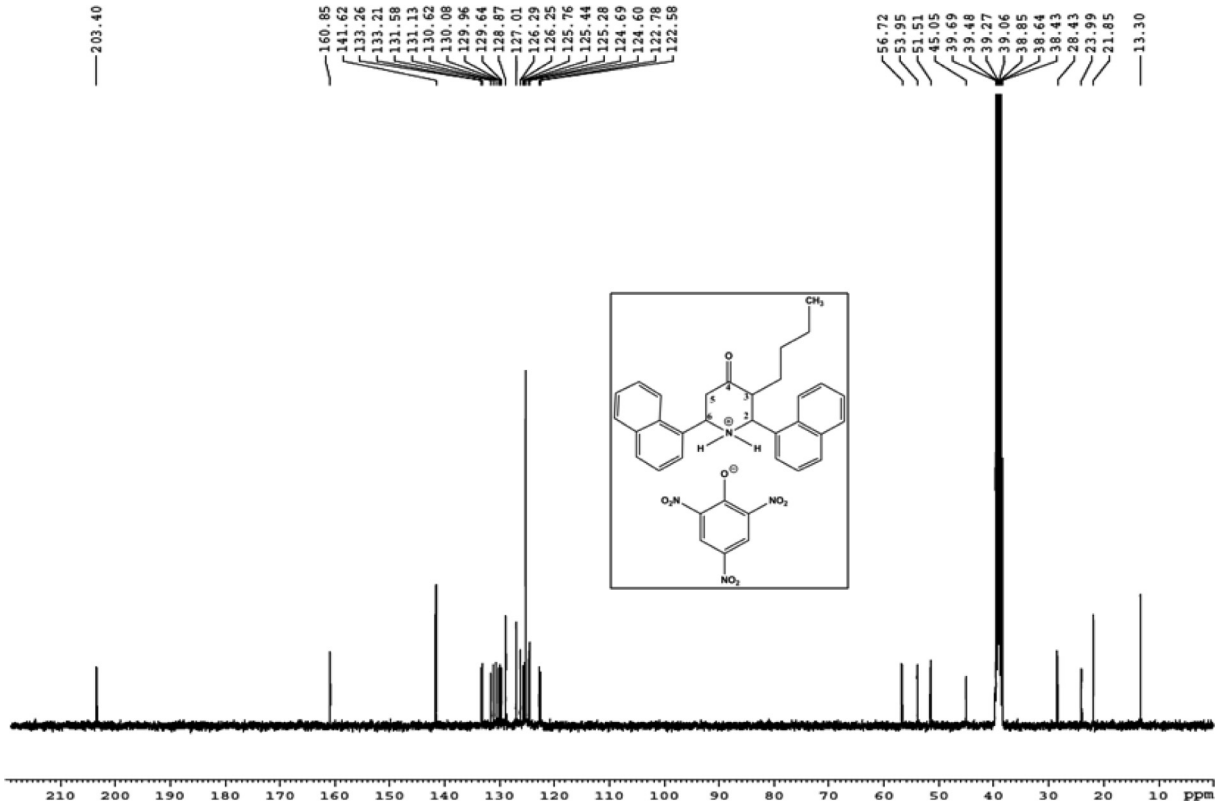

Fig. 4. ^{13}C NMR Spectrum of compound 4.

Table 7
Antibacterial and antifungal activities of compounds (1-6) by disc diffusion method.

Compound	Diameter of zone of inhibition (mm)								
	Bacterial strain					Fungal strain			
	E. coli	*S. aureus*	*B. subtilis*	*V. cholerae*	*P. aeruginosa*	*C. albicans*	*A. niger*	*A. flavus*	*T. Rubrum*
1	12	13	07	09	11	12	10	11	08
2	09	11	07	10	12	08	14	07	11
3	16	15	11	12	15	21	16	12	14
4	22	16	15	12	20	15	17	12	14
5	13	15	20	18	14	17	15	16	12
6	14	12	09	12	10	14	11	13	10
Ciprofloxacin	12	15	16	16	11	-	-	-	-
Amphotericin B	-	-	-	-	-	13	12	14	11

Table 8
Antibacterial and antifungal activities of compounds (1-6) by serial dilution method.

Compound	Minimum inhibitory concentration (μg/mL)								
	Bacterial strain					Fungal strain			
	E. coli	*S. aureus*	*B. subtilis*	*V. cholera*	*P. aeruginosa*	*C. albicans*	*A. niger*	*A. flavus*	*T. rubrum*
1	50	50	200	100	100	50	100	50	200
2	200	100	200	100	50	200	25	200	100
3	25	25	100	100	50	12.5	25	100	50
4	12.5	25	25	50	12.5	25	25	50	50
5	50	25	12.5	25	25	12.5	25	25	50
6	25	50	100	50	100	25	100	50	100
Ciprofloxacin	25	25	12.5	50	12.5	-	-	-	-
Amphotericin B	-	-	-	-	-	25	25	50	50

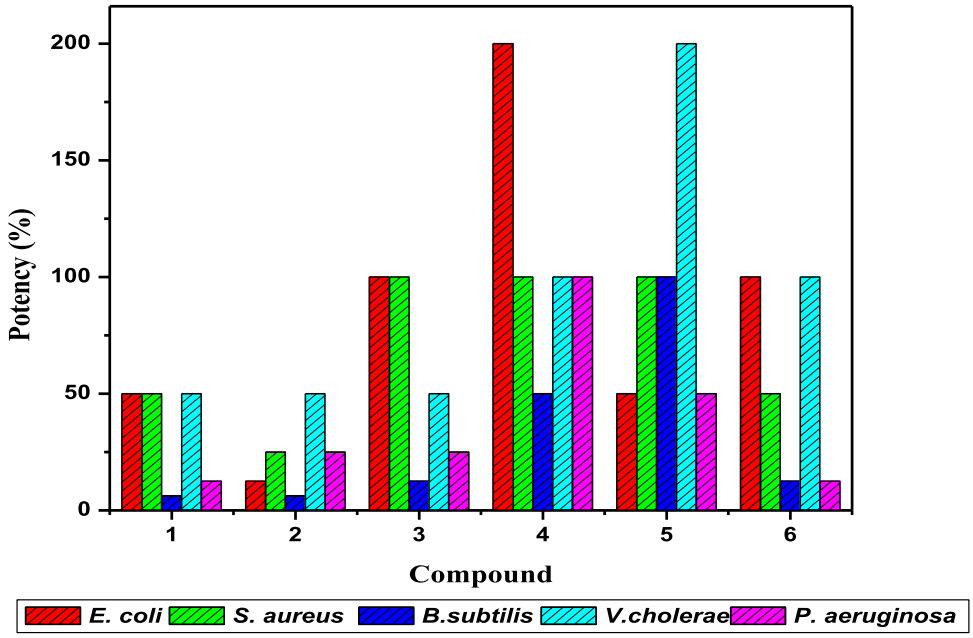

Fig. 5. Comparison of antibacterial potency of compounds (1–6).

bacterial strains are given in Tables 7 and 8. From the zone of inhibition, it is clear that the compounds **3, 4, 5** and **6** against *E. coli*, **3, 4** and **5** against *S. aureus* and *P. aeruginosa*, **5** against *B. subtilis* and *V. cholerea* is better in enhancing the anti-bacterial potency on the tested organisms than the others.

A close survey of the MIC values in Table 8 indicates that all the compounds exhibited a varied range 12.5-200 μg/mL of antibacterial activity against the tested bacterial strains. The compounds **1** and **2** were inactive against all the tested bacterial strains. The compound **3** with methyl groups at C-3 and C-5 positions of piperidone ring exhibited good activity against *E. coli* and *S. aureus* whereas against *B. subtilis, V. cholerae* and *P. aeruginosa* poor activity was noted. Introduction of butyl group at C-3 position of the piperdone moiety in **1** (compound **4**) exhibited excellent activity against all the tested bacterial strains except *B. subtilis*. Replacement of methyl groups by the pentyl group at C-3 and 1-naphthyl by the 2-naphthyl group in C-2 and C-6 positions of the piperidone ring in **1** (compound **5**) showed excellent activity against *S. aureus, B. subtilis* and *V. cholerae* while against *E. coli* and *P. aeruginosa* have registered poor activity. Substitution of the methyl group at C-3 and the 2-naphthyl group in C-2 and C-6 positions of the piperidone ring in **1** (compound **6**) displayed excellent activity against *E. coli* and *V. cholerae* but poor activity was noted against the rest of the tested bacterial strains.

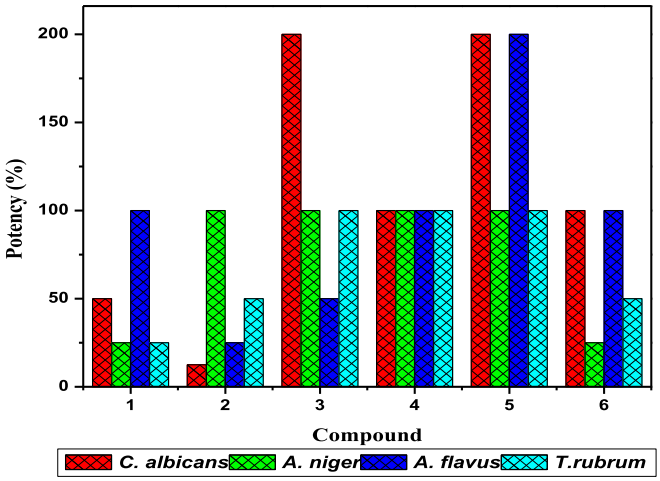

Fig. 6. Comparison of antifungal potency of compounds (1–6).

The zone of inhibition (mm) and minimum inhibitory concentrations (MIC in μg/mL) of the compounds (**1-6**) against the tested fungal strains are given in Tables 7 and 8. From the zone of inhibition, it is clear that the compounds **3, 4, 5** and **6** against *C. albicans* and *A. niger*, **5** against *A. flavus* and **3, 4, 5** against *T. rubrum* are found to be better in enhancing the antibacterial potency on the tested organisms than the others.

Table 8 shows the in vitro anti-fungal activities of compounds (**1-6**). Amphotericin B was used as standard drug on fungal strains such as *C. albicans, A. niger, A. flavus* and *T. rubrum*, whose activities were measured as the minimum inhibitory concentration (MIC in μg/mL). The compound with 1-naphthyl/2-naphthyl groups at C-2 and C-6 positions (**i.e. compounds 1-6**), compound **1** did not exert antifungal activity against *C. albicans, A. niger* and *T. rubrum* except *A. flavus*. Introduction of the isopropyl group at C-3 instead of the methyl group of piperidone moiety in **1**, (compound **2**) has good activity against *A. niger* whereas poor activity was noticed against all the tested fungal strains. However, further substitution of a methyl group at C-5 position in **1**, compound **3** has pronounced antifungal activity against *C. albicans, A. niger* and *T. rubrum* while against *A. flavus* poor activity was noted. Replacement of methyl groups by butyl group at C-3 position of piperidone moiety in **1** (compound **4**) showed excellent activity against all the tested fungal strains. Due to the incorporation of 2-naphthyl group at C-2 and C-6 and pentyl group at C-3 position of piperidone ring in **1** (compound **5**) exhibited excellent activity against all the fungal strains. Substitution of 2-naphthyl groups at C-2 and C-6 and further introduction of methyl group at C-5 position in **1** (compound **6**) has registered excellent activity against *C. albicans* and *A. flavus* while against *A. niger* and *T. rubrum* poor activity was noted.

The potency of synthesized compounds (**1-6**) against the tested bacterial and fungal strains was derived in comparison with the reference standards by using the following equation

$$\text{Potency (\%)} = \frac{\text{MIC } (\mu\text{g/mL}) \text{ of reference compound}}{\text{MIC } (\mu\text{g/mL}) \text{ of reference compound}} \times 100$$

The obtained results are also presented as shown in Figs. 5 and 6. On comparison with Ciprofloxacin, double the potency (200%) is noted for compound 4 against *E. coli* and compound **5** against *V. cholerae* while equal potency (100%) is noted for compounds **3** and **6** against *E. coli*, compound **5** against *B. subtilis*, **3, 4, 5** against

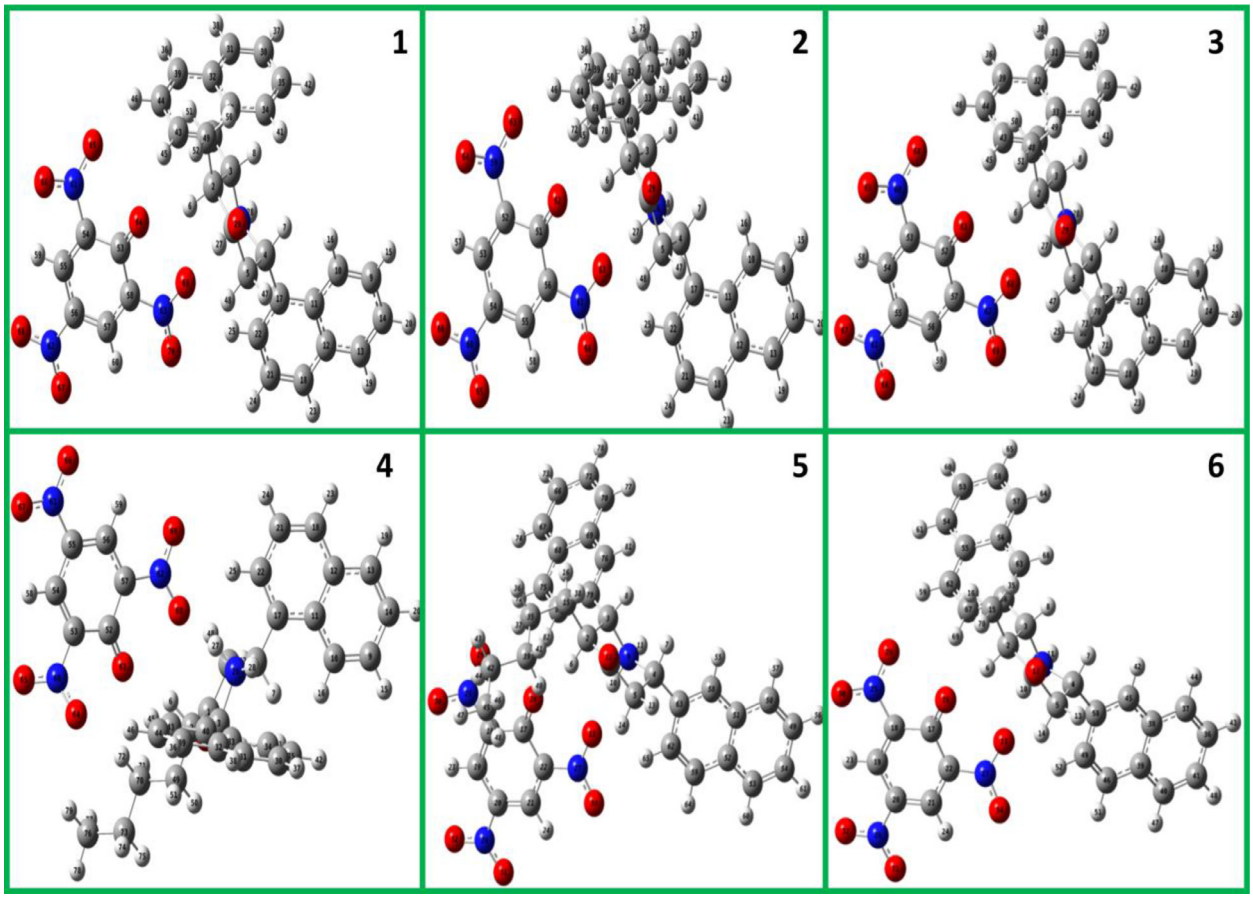

Fig. 7. Optimized molecular structures of compounds (1-6) by B3LYP/6-311++G(d,p) method.

Table 9
Selected bond lengths, bond angles and dihedral angles of compounds (1-6).

Bond Lengths (Å)	1	2	3	4	5	6
C1-C2	1.535	1.535	1.536	1.534	1.536	1.537
C2-C3	1.551	1.556	1.550	1.554	1.554	1.549
C3-N9	1.556	1.555	1.552	1.557	1.557	1.555
N9-C4	1.535	1.533	1.536	1.535	1.543	1.546
C4-C5	1.540	1.538	1.552	1.541	1.539	1.538
C1-C5	1.525	1.528	1.538	1.526	1.528	1.528
C17-O28	1.262	1.263	1.262	1.263	1.264	1.264
C17-C22	1.472	1.471	1.472	1.471	1.468	1.469
C17-C18	1.469	1.468	1.469	1.468	1.466	1.467
C22-C21	1.398	1.397	1.397	1.399	1.398	1.397
C18-C19	1.371	1.371	1.371	1.371	1.373	1.373
N9-H10	1.046	1.045	1.045	1.045	1.043	1.044
N9-H11	1.026	1.026	1.026	1.026	1.025	1.025
Bond Angles (°)	**1**	**2**	**3**	**4**	**5**	**6**
C2-C1-C5	117.92	117.93	118.53	117.48	117.42	118.09
C1-C2-C3	110.72	110.76	110.33	109.89	109.43	110.27
C1-C5-C4	112.03	112.58	109.71	111.30	111.90	112.66
C17-C22-C21	122.51	122.46	122.52	122.48	122.65	122.83
C17-C18-C19	123.77	123.75	123.75	123.73	123.65	123.61
C22-C17-C18	112.61	112.66	112.60	112.70	112.81	112.75
O33-N27-O34	120.12	120.19	120.17	120.19	120.13	119.96
O31-N26-O32	123.80	123.80	123.79	123.80	123.81	123.81
O29-N25-O30	123.60	123.65	123.58	123.59	123.50	123.36
Dihedral Angles (°)	**1**	**2**	**3**	**4**	**5**	**6**
N9-C4-C5-C1	-54.1	-54.1	-54.0	-54.9	-53.9	-52.5
C5-C1-C2-C15	-169.2	-170.7	-171.6	-173.0	-173.4	-169.1
N9-C3-C2-C15	173.5	177.2	173.9	175.3	178.9	177.7
N9-C3-C2-C1	49.8	49.0	50.6	50.9	53.7	53.3
C50-C4-C5-C1	-178.1	-178.0	-177.5	-179.0	-179.3	-178.8
C1-C2-C3-C66	172.9	171.1	173.4	173.0	173.2	173.0
H10-N9-C4-C5	-56.1	-56.1	-56.2	-56.7	-56.3	-55.5
H10-N9-C3-C2	57.7	58.0	58.3	58.3	55.2	55.6
H11-N9-C4-C5	-174.7	-174.6	-174.3	-175.0	-174.6	-173.5
H11-N9-C3-C2	175.2	175.3	175.5	175.5	175.0	175.5

S. aureus, **4, 6** against *V. cholerae*, **4** against *P. aeruginosa*. But, the remaining compounds exert lesser potentially in the range 6.25-50% than the standard drug. With reference to *Amphotericin B*, an equal potency is noted for compounds **4** and **6** against *C. albicans*, **2, 3, 4** and **5** against *A. niger*, **1, 4** and **6** against *A. flavus*, **3, 4** and **5** against *T. rubrum* while compounds **3** and **5** against *C. albicans* and **5** against *A. flavus* are doubly effective. But 12.5-50% potency is noted with the rest of the compound when compared to the standard drug.

3.4. DFT study

Geometry optimizations for the compounds (**1-6**) were carried out according to DFT/6-311++G(d,p) basis set by using Gaussian-09W program package [24]. The optimized molecular structures of (**1-6)** are shown in Fig. 7.

The selected bond lengths, bond angles and dihedral angles values are given in Table 9. In the picrate anion, the C-O bond distance of the anion shows characteristic value with O28-C17 (~1.26) Å) which is intermediate between single and double bond lengths. The loss of a proton from picric acid is confirmed by the lengthening of the C-C bond. The C17-C22 and C17-C18 bond length of ~1.47 Å deviate from the standard aromatic C-C bond lengths (1.40 Å). These differences are attributed to the loss of a hydroxyl proton of picric acid, leading to conversion from the neutral to the anionic state where the negative charge is constrained to lie in the ring.

The repulsive interactions of the deprotaneted oxygen atom with the electron withdrawing NO_2 groups attached to the *ortho* positions are responsible for the shortening of the C22-C21 ~1.39 Å and C18-C19 ~1.37 Å bonds as well as for the significant difference between the internal C-C-C angles within the ring. Both C-C-C angles joining the NO_2 groups C17-C22-C21, 122.83° and C17-C18-C19, 123.61° are significantly greater and C22-C17-C18, 112.75° angles joining the deprotonated hydroxyl group is significantly smaller than the expected angle (120°) for sp^2 hybridized carbon. On comparison, of bond lengths of C17-C22, ~1.47 Å, C17-C18, ~1.46 Å, C22-C21 ~1.39 Å, C18-C19 ~1.37 Å and C-O, ~1.26 Å with normal bond lengths of C-C, C=C and C-O, it is found that C17-C22, C17-C18 (1.4 Å) have single bond character and C22-C21,

Table 10
HOMO-LUMO energies and dipole moments of compounds (1-6).

Compound	HOMO-LUMO Energies (eV)			Dipole Moment			
	HOMO	LUMO	ΔE	μ_x	μ_y	μ_z	μ_{tot}
1	-6.5437	-3.4268	3.1169	15.3904	2.884	-3.8793	16.1317
2	-6.5557	-3.4268	3.1289	15.3634	2.1482	-4.2466	16.0836
3	-6.5220	-3.3768	3.1452	15.472	2.8185	-3.6523	16.1452
4	-6.5565	-3.4295	3.1270	15.2047	-2.3043	4.0525	15.9033
5	-6.4341	-3.4116	3.0225	13.8393	7.3006	-1.4985	15.7185
6	-6.4036	-3.3871	3.0165	13.6338	7.0495	-2.7717	15.5967

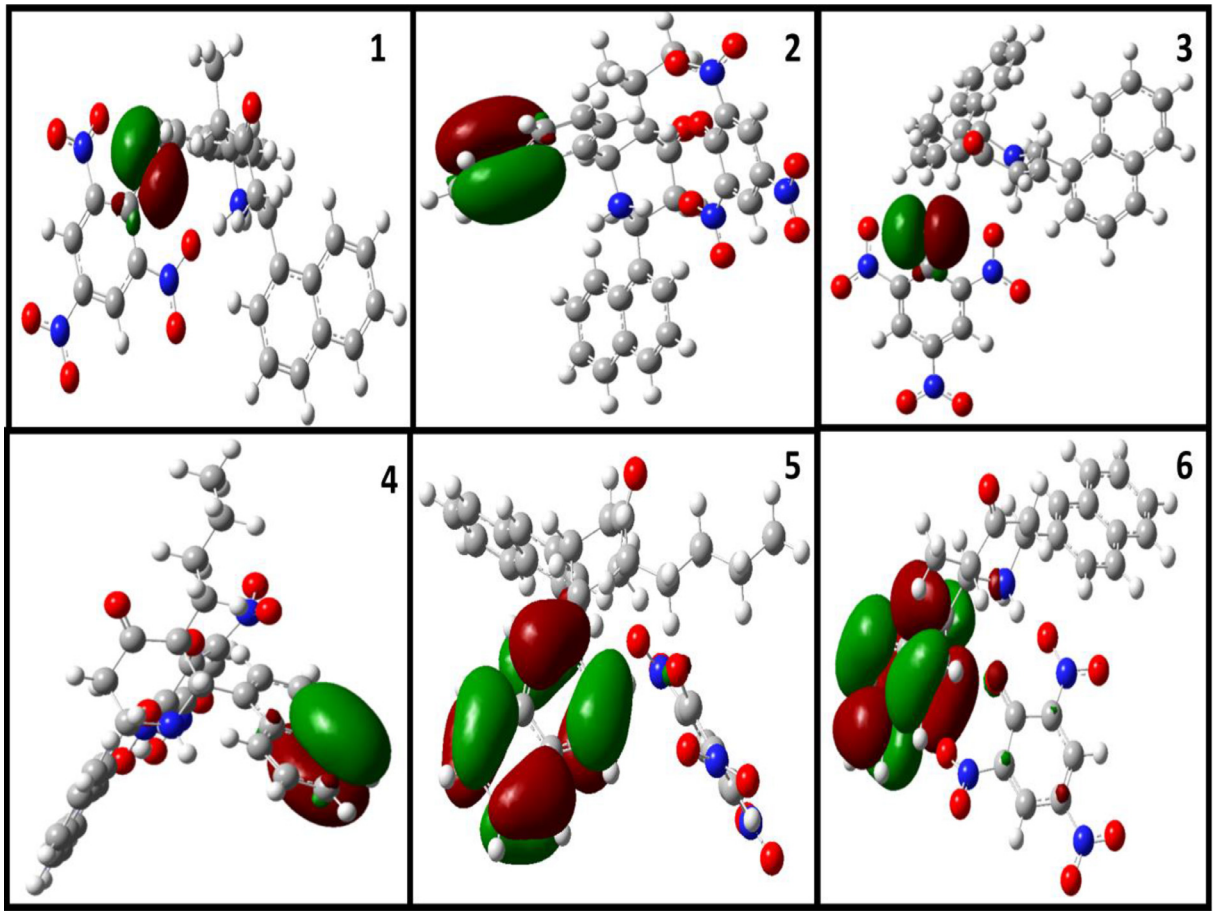

Fig. 8. HOMO energies of compounds (1-6).

C18-C19 (1.39 Å) have double bond character. The C-O (1.21 Å) also carries the double bond character. This indicates that the complex possesses more quinonoid than benzenoid character.

An equatorial orientation of the naphthyl group is witnessed by its torsional angles ~170.0° [C5-C1-C2-C15] and ~177.3° [N9-C3-C2-C15]. The torsional angles of the naphthyl groups on both sides of the amino group are -178.8° [C50-C4-C5-C1] and -173.0° [C1-C2-C3-C66], which support the equatorial orientation of the naphthyl groups. The N-atom of the piperidone molecule shows sp^3 hybridization, which can be noticed from the angles around that nitrogen. The N9-H10 group also adopts an equal disposition to the best plane of the piperdone ring, which is evidenced from the torsional angles H11-N9-C4-C5= -173.5° and H11-N9-C3-C2= 175.5° and H10-N9-C4-C5= -55.5° and H10-N9-C3-C2= 55.6°.

HOMO-LUMO energies have been determined theoretically according to DFT calculations using B3LYP/6-311++G(d,p) level of theory. From the HOMO-LUMO orbital picture (Figs. 8 and 9) it was found that in compounds **6** and **5**, the HOMO is located on the C-O^- group in picric acid, whereas the LUMO is located on the Nitro group at the *para* position in picric acid. In compounds **1** and **3**, the HOMO is located on the naphthyl group attached to C1 carbon in piperidine moiety, whereas the LUMO is located on the Nitro group at the *para* position in picric acid. In compounds **2** and **4**, the HOMO is located on the naphthyl group attached to C1 in piperidine moiety, whereas the LUMO is located on the phenolic oxygen in picric acid. It is seen from Table 10, the replacement of 2-naphthyl group by1-naphthyl group at C1 and C5 in piperidine ring moiety increases the energy gap and bulkiness of alkyl group at C3 position also influences the energy gap. The HOMO-LUMO transition implies that intra-molecular charge transfer takes place within the molecule. All the synthesized compounds (**1-6**) with the lowering of HOMO- LUMO band gap and lower dipole moment exhibits higher bioactive properties of the molecule against the both tested bacterial and fungal strains.

In order to predict the electron density of nitrogen and oxygen performed by DFT calculations and obtained MEP for compounds **1-6**. MEP surface diagram (Fig. 10) Is used to understand the reactive sites in of a molecule. The MEP images of compounds **1-6** clearly suggest that oxygen and nitrogen atoms represent the nucleophilic center (dark red), whereas the protonated nitrogen bears positive charge. The MEP clearly confirms the existence of the electrophillic active centers characterized by red colour.

The density functional theory has been used to calculate the dipole moment (μ), mean polarizability (α) and the total first static hyperpolarizability (β_0) for **1-6** in terms of *x, y, z* components and is given by the following equations.

$$\mu = \left(\mu_x{}^2 + \mu_y{}^2 + \mu_z{}^2\right)^{1/2}$$

$$\alpha_{tot} = \frac{1}{3}(\alpha_{xx} + \alpha_{yy} + \alpha_{zz})$$

$$\Delta\alpha = \frac{1}{\sqrt{2}}\Big[\left(\alpha_{xx} - \alpha_{yy}\right)^2 + \left(\alpha_{yy} - \alpha_{zz}\right)^2 + (\alpha_{zz} - \alpha_{xx})^2 + 6\left(\alpha_{xy}^2 + \alpha_{yz}^2 + \alpha_{xz}^2\right)\Big]^{\frac{1}{2}}$$

$$\beta_0 = \Big[(\beta_{xxx} + \beta_{xyy} + \beta_{xzz})^2 + (\beta_{yyy} + \beta_{xxy} + \beta_{yzz})^2 + (\beta_{zzz} + \beta_{xxz} + \beta_{yyz})^2\Big]^{1/2}$$

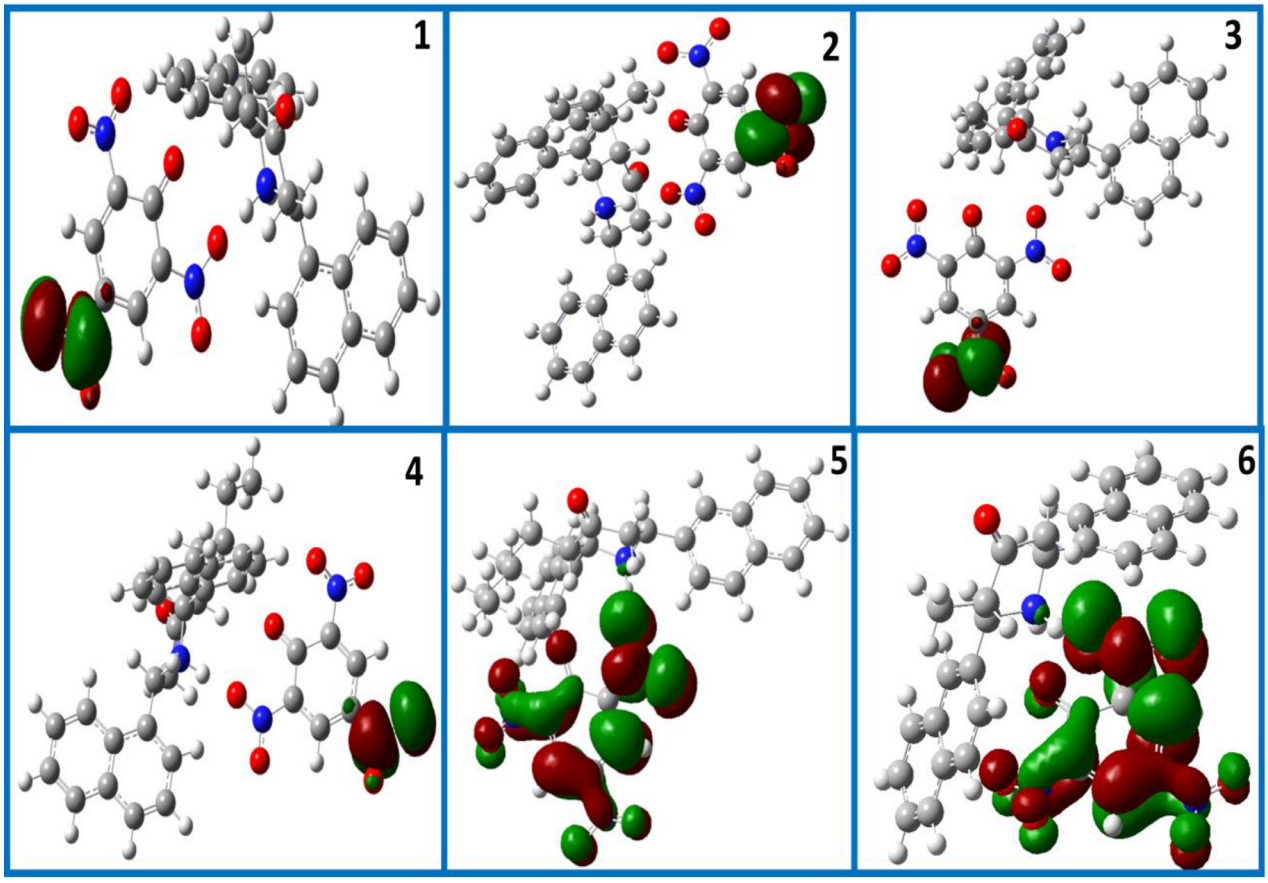

Fig. 9. LUMO energies of compounds (1-6).

Table 11
Polarizability and first hyperpolarizability of compounds (1-6).

Compound	1	2	3	4	5	6
α_{xx}	281.98	295.67	292.02	293.71	282.96	269.49
α_{yy}	256.82	276.34	262.46	295.76	291.72	263.16
α_{zz}	267.72	272.69	272.63	271.04	295.11	267.63
α_{xy}	-13.53	-16.95	-12.93	20.67	-13.65	-17.37
α_{xz}	-8.77	-8.37	-10.29	7.51	-10.60	-8.91
α_{yz}	-18.43	-18.14	-19.26	-18.34	-23.64	-15.79
α_o(x10^{-23}) (esu)	3.98	4.2	4.09	4.25	4.30	3.95
$\Delta\alpha$ (x10^{-24}) (esu)	6.73	7.55	7.20	8.49	7.74	6.47
β_{XXX}	645.3052	649.4835	650.8677	621.6441	514.2514	500.5509
β_{YYY}	42.1811	24.2724	47.4182	-59.8622	227.5143	221.4778
β_{ZZZ}	-87.1668	-97.1635	-72.0881	128.2878	-91.2742	-85.8137
β_{XYY}	131.0622	163.4085	123.7093	198.1327	164.6443	164.2975
β_{XXY}	53.6178	55.5242	64.07	-72.6862	60.0789	100.2613
β_{XXZ}	9.9549	9.7643	2.3299	-19.2332	16.2086	-42.7065
β_{XZZ}	-7.0948	-29.3598	3.9566	-51.7681	-24.9955	-30.4014
β_{YZZ}	34.0308	42.5668	24.866	-23.9767	69.1207	13.8675
β_{YYZ}	-37.8465	-25.0478	-36.882	-3.9599	30.3782	-3.467
β_{XYZ}	105.3365	82.8687	110.0518	38.2465	120.0581	118.7922
β_{tot} (x10^{-30}) (esu)	6.8100	6.92	6.8900	6.8300	6.4467	6.3048

All the electric dipole moments and first hyperpolarizabilities were calculated by taking the origin of the Cartesian coordinate system (x,y,z) = (0,0,0) at the center of mass of the compounds.

The dipole moment (μ), mean polarizability (α) and the total first static hyperpolarizability (β_0) are related directly to the non-linear optical efficiency of structures. The optical non-linearity of organic materials originates from the delocalized electron cloud of the substituent groups. All the compounds (**1-6**) are found to be polar molecules and have non-zero dipole moment components. Introduction of the smaller alkyl group at C3 slightly enhances the dipole moment, whereas bulky alkyl group decreases the dipole moment. Non – zero dipole moments result in large microscopic first hyperpolarizabilities and hence, have a good microscopic NLO behavior.

The calculated polarizabilities α_{tot} have non-zero values and are dominated by diagonal components. As seen from Table 11, β_{tot} values for 1-naphthyl substituted piperidone picrates (**1-4**) are higher than that of 2-naphthyl substituted derivatives (**5** and **6**). In compounds **5** and **6** as buliknes of alkyl group at C2 increases, β_{tot} values also increase, whereas in compounds (**1-4**), the NLO charac-

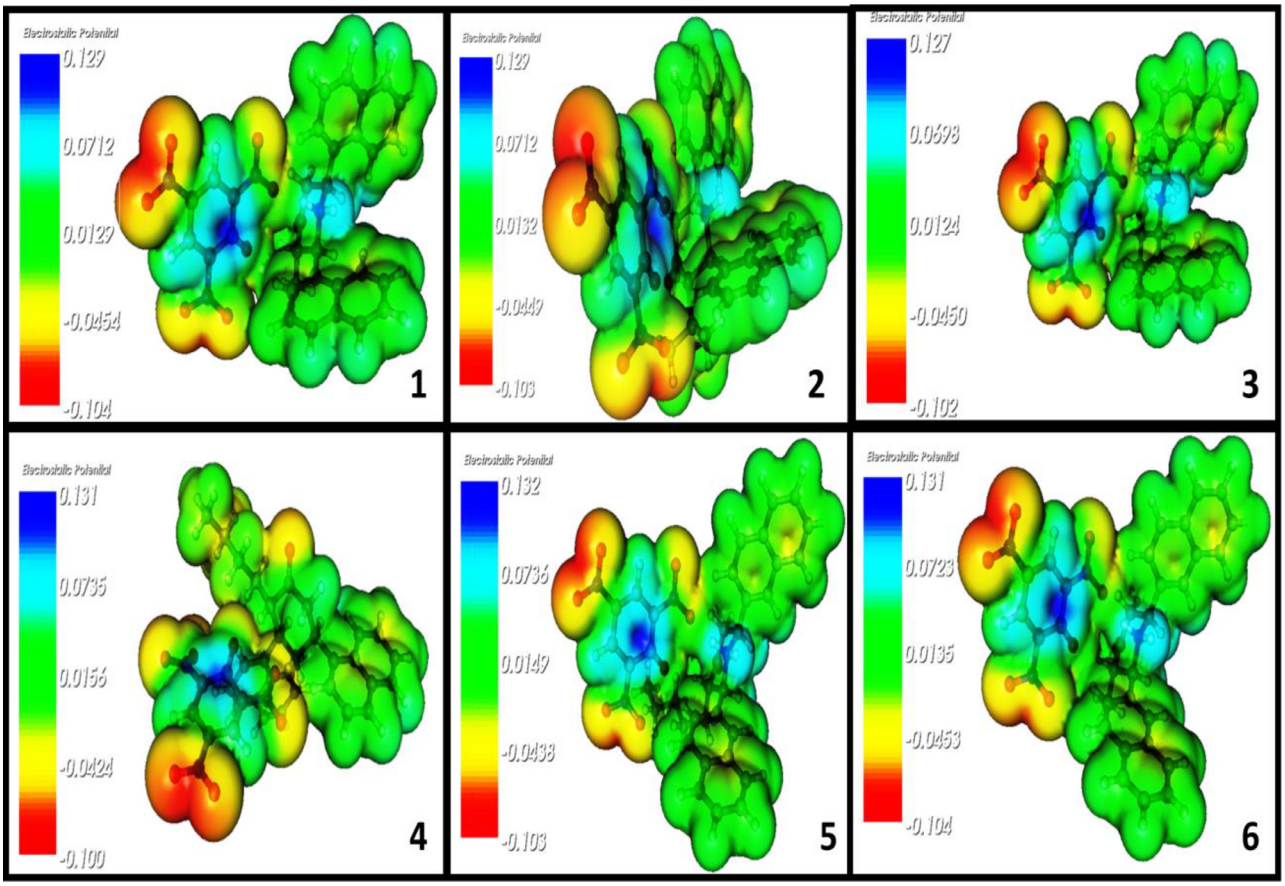

Fig. 10. MEP diagram of compounds (1-6).

Table 12
Hydrogen bond interactions of piperidone with amino acids at the active site of Acetylcholinesterase Inhibitors of compounds (1-6).

Compound	Docking Score	Hydrogen Bonding Interactions Donor	Acceptor	Distance (Å)
1	-14.1	-	-	-
2	-11.7	**TYR129(N-H…O)**	O*	2.9
3	-11.9	-	-	-
4	-10.6	**PHE287(O…H-N)PHE330(O-H…O)**	N*O*	3.13.3
5	-11.2	**TYR129(O-H…O)**	O*	2.8
6	-12.4	**ARG288(N-H…O)(O-H…O)ILE286(N-H…O)**	O*O*O*	3.33.22.8
Co-Crystal (**1-BENZYL-4-[(5,6-DIMETHOXY-1-INDANON-2-YL)METHYL]PIPERIDINE**)	-10.4	**THR129(O…H-N)**	N*	2.6

* Ligand

ter decreases according to the following order C2-CH(CH_3)$_2$ (**2**) > C2 & C4- CH_3 (**3**) > C2-CH_3 (**1**) > C2-(CH_2)$_3$$CH_3$ (**4**).

3.5. Molecular docking studies

The entire docking calculations were performed using the Autodock docking module program. It performs flexible protein-ligand docking and searches for favorable interactions between one typically small ligand molecule and a typically larger protein molecule. Docking process, wherein the protein preparation inhibited refinement is carried out with a maximum of 20 poses, wherein the side chains are optimized and refinement of residues takes place, if the ligand poses are within 5.0Å. The best docked structure was chosen by docking score and the number of amino acids matches (hydrogen bonds) with original drug complex.

The docked, glide energy and hydrogen bonding interactions of the compounds (**1-6**) and co-crystallized ligand is given in Table 12. A view of the X-ray crystal structure of the title compound in the Acetylcholinesterase Inhibitors Receptor active site showing the key hydrogen contacts between inhibitor and enzyme is depicted in Figs 11(a-f). The surface diagram showing the compounds (**1-6**) docked at the active site of Acetylcholinesterase Inhibitors Receptor is depicted in Fig. 12. Molecular analysis of compounds **(1-6)** indicated that hydrogen bond and hydrophobic are four major interactions (THR9, VAL12, GLN20) incorporating the attachment of this ligand to Acetylcholinesterase Inhibitors acceptor. The co-crystallized ligand also docked well and it shows better interactions with active residues. The results show that the compound **1** having better binding energy and the co-crystallized ligand have comparable interactions. It is indicated that compound **6** has better ligand protein interactions. X-ray crystal structures confirmed the expected binding mode, and consideration of binding orientation and electronic properties enabled optimization to Piperidone as a more potent second-generation lead.

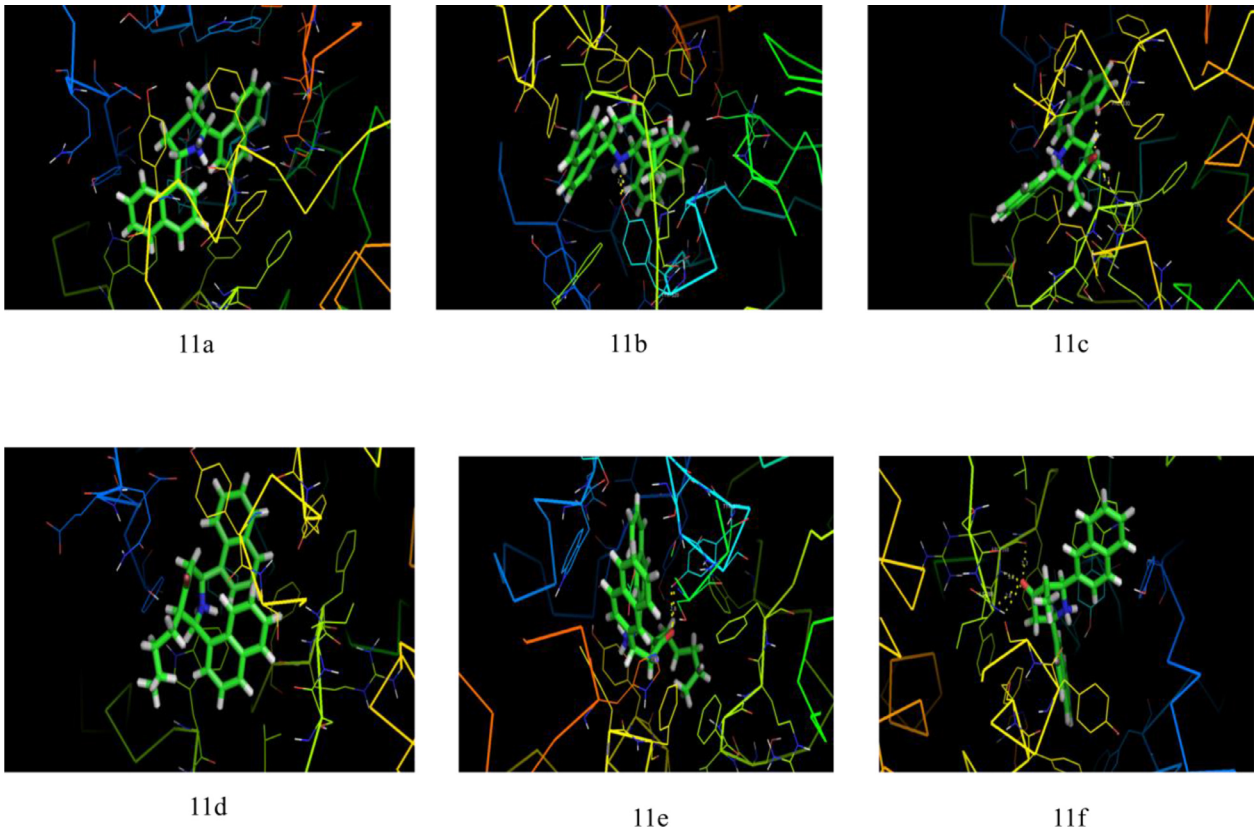

Fig. 11. (a-f) The title compounds (1-6) in the Acetylcholinesterase Inhibitors Receptor active site showing key hydrogen contacts between piperidone inhibitor and enzyme.

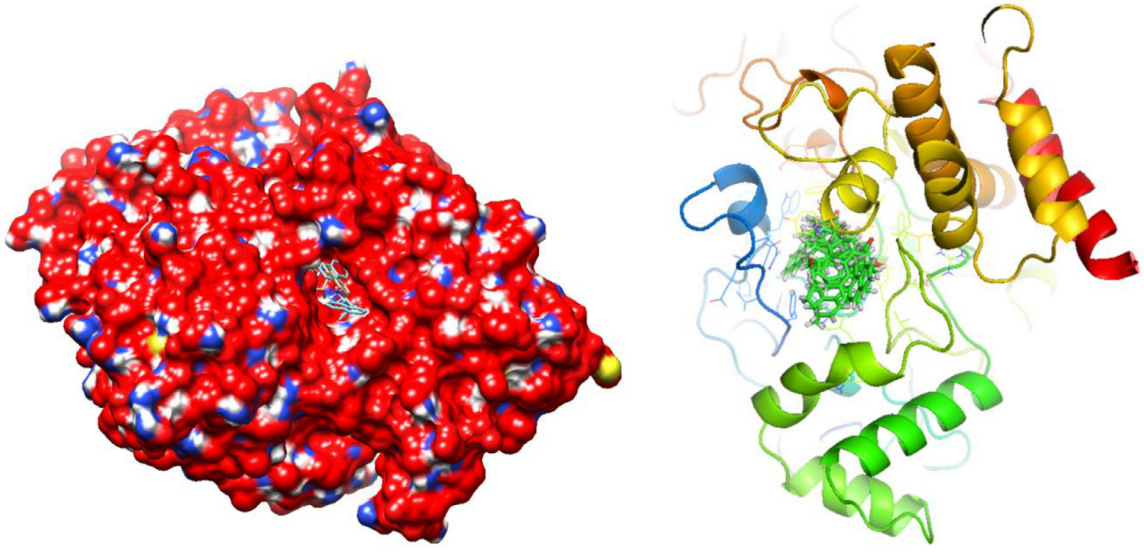

Fig. 12. Surface and Cartoon diagram showing the piperidone docked at the active site of Acetylcholinesterase Inhibitors.

4. Conclusions

A series of 3-alkyl/3,5-dialkyl-2r,6c-di(naphthyl)piperidin-4-one picrates have been synthesized successfully in appreciable yields and were characterized by elemental analysis, FT-IR, Mass, 1D (^{1}H and ^{13}C), and 2D (HOMOCOSY, HSQC, HMBC, NOESY, and DEPT) NMR spectral techniques. The NMR spectral data suggest that the title compounds (**1-6**) exist in normal chair conformation with equatorial orientation of all the substitutes. Due to protonation, the axial N-H bond experiences severe syn 1,3-diaxial interaction with axial hydrogens at C-3 and C-5 and due to these interactions the protons H-3a and H-5a are deshielded and corresponding carbons C-3 and C-5 shielded. The chemical shifts of the heterocyclic ring protons are influenced by the picrate anion. All the newly synthesized compounds were screened for their antibacterial and antifungal activities. Most of the compounds showed good antibacterial and antifungal activities. However, the antibacterial and antifungal activities are significantly influenced by the aromatic substituents. The geometry optimization have been obtained for the compounds (**1-6**) by using DFT/B3LYP/6-311++G(d,p) level. The lowering of

HOMO and LUMO energy gap clearly indicates the charge transfer taking place within the molecule. The MEP maps show that oxygen and nitrogen atoms are the negative potential sites and the positive potential sites are around the hydrogen atoms. The total dipole moment, polarizability and hyperpolarizability of the compounds were calculated and the results show that the molecule could be good NLO material. Docking results show that the compound **1** having better binding energy and the co-crystallized ligand have comparable interactions. It is indicated that compound **6** has better ligand protein interactions.

Author contribution statement

S. Savithiri: Conceived and designed the experiments; Performed the experiments; Analyzed and interpreted the data; Contributed reagents, materials, analysis tools or data; Wrote the paper.

S. Bharanidharan: Conceived and designed the experiments; Contributed reagents, materials, analysis tools or data.

P. Sugumar: Performed the experiments; Analyzed and interpreted the data.

C. Rajeevgandhi: Analyzed and interpreted the data.

M. Indhira: Analyzed and interpreted the data.

Declaration of Competing Interest

The authors declare no conflict of interest.

Supplementary materials

Supplementary material associated with this article can be found, in the online version, at doi:10.1016/j.molstruc.2021.130145.

References

[1] P. Parthiban, S. Balasubramanian, G. Aridoss, S. Kabilan, Spectrochim. Acta. A. 70 (2008) 1–24.
[2] C. Ramalingam, Y.T. Park, S. Kabilan, Eur. J. Med. Chem. 41 (2006) 683–696.
[3] I.G. Mokio, A.T. Soldatenkov, V.O. Federov, E.A. Ageev, N.D. Sergeeva, S. Lin, E.E. Stashenku, N.S. Prostakov, E.L. Andreeva, Khim Farm Zh 23 (1989) 421–427.
[4] P. Parthiban, G. Aridoss, P. Rathika, V. Ramkumar, S. Kabilan, Bioorg. Med. Chem. Lett. 19 (2009) 2981–2985.
[5] H.I. El-Subbagh, S.M. Abu-Zaid, M.A. Mahran, F.A. Badria, A.M. Al-Obaid, J. Med. Chem. 43 (2000) 2915–2921.
[6] A.A. Watsona, G.W.J. Fleet, N. Asano, R.J. Molyneux, R.J. Nugh, Phytochemistry 56 (2001) 265–295.
[7] G. Aridoss, S. Amirthaganesan, M.S. Kim, J.T. Kim, Y.T. Jeong, Eur. J. Med. Chem. 44 (2009) 4199–4210.
[8] E.L. Eliel, M.H. Gianni, T.H. Williams, J.B. Stothers, Tetrahedron Lett 3 (17) (1962) 741–747.
[9] N.S. Bhacca, D.H. Williams, Applications of NMR Spectroscopy in Organic Chemistry: Illustration from the Steroid Field, Holden-Day, 1964.
[10] H. Booth, J.H. Little, Tetrahedron 23 (1) (1967) 291–297.
[11] A. Manimekalai, J. Jayabharathi, Ind. J. Chem. 45B (2006) 1686–1691.
[12] V. Vimalraj, K. Pandiarajan, Magn. Reson. Chem. 49 (10) (2011) 682–687.
[13] Z. Dega-Szafran, G. Dutkiewicz, Z. Kosturkiewicz, M. Petryna, J. Mol. Struct. 708 (1-3) (2004) 15–21.
[14] V. Stilinović, B. Kaitner, Cryst. Growth & Design 11 (9) (2011) 4110–4119.
[15] B. Bashir, B. Zhang, S. Pan, Z. Yang, J. Alloys and Compounds 758 (2018) 85–90.
[16] C. Zhang, Y. Song, X. Wang, Coord. Chem. Rev. 251 (1-2) (2007) 111–141.
[17] T. Arivazhagan, S.S.B. Solanki, N.P. Rajesh, J. Cryst. Growth 496 (2018) 43–50.
[18] V. Ramesh, K. Rajarajan, Appl. Phy. B. 113 (1) (2013) 99–106.
[19] M.M. Chen, H.G. Xue, S.P. Guo, Coord. Chem. Rev. 368 (2018) 115–133.
[20] G.A. Babu, S. Sreedhar, S.V. Rao, P. Ramasamy, J. Cryst. Growth 312 (12-13) (2010) 1957–1962.
[21] B. Dhanalakshmi, S. Ponnusamy, C. Muthamizhchelvan, J. Cryst. Growth 313 (1) (2010) 30–36.
[22] S. Savithri, M. Arockia doss, G. Rajarajan, V. Thanikachalam, J. Mol. Struct. 1105 (2015) 225–237.
[23] S. Savithiri, M. Arockia doss, G. Rajarajan, V. Thanikachalam, J. Mol. Struct. 1075 (2014) 430–441.
[24] M.J. Frisch, G.W. Trucks, H.B. Schlegel, G.E. Scuseria, M.A. Robb, J.R. Cheeseman, G. Scalmani, V. Barone, B. Mennucci, G.A. Petersson, H. Nakatsuji, M. Caricato, X. Li, H.P. Hratchian, A.F. Izmaylov, J. Bloino, G. Zheng, J.L. Sonnenberg, M. Hada, M. Ehara, K. Toyota, R. Fukuda, J. Hasegawa, M. Ishida, T. Nakajima, Y. Honda, O. Kitao, H. Nakai, T. Vreven, J.A. Montgomery Jr., J.E. Peralta, F. Ogliaro, M. Bearpark, J.J. Heyd, E. Brothers, K.N. Kudin, V.N. Staroverov, T. Keith, R. Kobayashi, J. Normand, K. Raghavachari, A. Rendell, J.C. Burant, S.S. Iyengar, J. Tomasi, M. Cossi, N. Rega, J.M. Millam, M. Klene, J.E. Knox, J.B. Cross, V. Bakken, C. Adamo, J. Jaramillo, R. Gomperts, R.E. Stratmann, O. Yazyev, A.J. Austin, R. Cammi, C. Pomelli, J.W. Ochterski, R.L. Martin, K. Morokuma, V.G. Zakrzewski, G.A. Voth, P. Salvador, J.J. Dannenberg, S. Dapprich, A.D. Daniels, O. Farkas, J.B. Foresman, J.V. Ortiz, J. Cioslowski, D.J. Fox, Gaussian 09, 2010 Revision C.02, Gaussian Inc., Wallingford CT.
[25] G. Kryger, I. Silman, J.L. Sussman, Struct. 7 (1999) 297–307.
[26] Z. Bikadi, E. Hazai, J. Chem info. 1 (1) (2009) 15.
[27] G.M. Morris, D.S. Goodsell, R.S. Halliday, R. Huey, W.E. Hart, R.K. Belew, A.J. Olson, J. Comp. Chem. 19 (1998) 1639–1662.
[28] M. Arockia doss, S. Savithiri, S. Vembu, G. Rajarajan, V. Thanikachalam, Can. Chem. Trans. 3 (2015) 261–274.